



Title	Molecular dynamic simulation of damage formation at Si vertical walls by grazing incidence of energetic ions in gate etching processes
Author(s)	Mizotani, Kohei; Isobe, Michiro; Hamaguchi, Satoshi
Citation	Journal of Vacuum Science and Technology A: Vacuum, Surfaces and Films. 2015, 33(2), p. 021313
Version Type	VoR
URL	<a href="https://hdl.handle.net/11094/78466">https://hdl.handle.net/11094/78466</a>
rights	This article may be downloaded for personal use only. Any other use requires prior permission of the author and AIP Publishing. This article appeared in Journal of Vacuum Science & Technology A 33, 021313 (2015) and may be found at <a href="https://doi.org/10.1116/1.4907724">https://doi.org/10.1116/1.4907724</a> .
Note	

*The University of Osaka Institutional Knowledge Archive : OUKA*

<https://ir.library.osaka-u.ac.jp/>

The University of Osaka

# Molecular dynamic simulation of damage formation at Si vertical walls by grazing incidence of energetic ions in gate etching processes

Cite as: J. Vac. Sci. Technol. A **33**, 021313 (2015); <https://doi.org/10.1116/1.4907724>

Submitted: 12 September 2014 . Accepted: 26 January 2015 . Published Online: 24 February 2015

Kohei Mizotani, Michiro Isobe, and Satoshi Hamaguchi



View Online



Export Citation



CrossMark

## ARTICLES YOU MAY BE INTERESTED IN

[Overview of atomic layer etching in the semiconductor industry](#)

Journal of Vacuum Science & Technology A **33**, 020802 (2015); <https://doi.org/10.1116/1.4913379>

[Plasma etching: Yesterday, today, and tomorrow](#)

Journal of Vacuum Science & Technology A **31**, 050825 (2013); <https://doi.org/10.1116/1.4819316>

[Classical interatomic potentials for Si-O-F and Si-O-Cl systems](#)

The Journal of Chemical Physics **115**, 6679 (2001); <https://doi.org/10.1063/1.1400789>



Advance your science and  
career as a member of  
**AVS**

LEARN MORE



# Molecular dynamic simulation of damage formation at Si vertical walls by grazing incidence of energetic ions in gate etching processes

Kohei Mizotani, Michiro Isobe, and Satoshi Hamaguchi<sup>a)</sup>

Center of Atomic and Molecular Technologies, Osaka University, 2-1 Yamadaoka, Suita, Osaka 565-0871, Japan

(Received 12 September 2014; accepted 26 January 2015; published 24 February 2015)

During gate etching processes of multigate fin-type field effect transistors (finFETs), energetic ions may hit the vertical walls at grazing angles and form damaged layers there. Such damages, if formed, can affect the device performance since part of the Si vertical walls of a finFET structure is used as a conductive channel. In this article, possible damage formation mechanisms at a Si vertical wall by energetic incidence of hydrogen ions ( $H^+$ ) and other heavier ions are discussed based on molecular dynamics simulation. In typical plasma processing conditions, incident ions are highly directional toward the wafer surface and therefore ions that hit such a vertical wall do so only at nearly grazing angles. It has been found in this study that the penetration depth of  $H^+$  into a Si substrate is weakly dependent on the incident angle and therefore ions at grazing incidence can form deep damage. The results indicate that, in gate etching processes with HBr plasmas or other plasmas with hydrogen, control of energetic hydrogen ion bombardment is critical in minimizing possible surface damage at Si vertical walls. © 2015 American Vacuum Society.

[<http://dx.doi.org/10.1116/1.4907724>]

## I. INTRODUCTION

Planer metal oxide semiconductor field effect transistor (MOSFET) technologies are reaching their limit of down scaling<sup>1–5</sup> whereas further integration of transistors with ever higher packing densities is still demanded by the market. Multigate field effect transistors (FETs), which can suppress short-channel effects of planer MOSFETs, have been adopted as a leading approach to integrate more transistors in a single chip. Among various multigate FETs, fin-type FETs (finFETs) use fin structures as their gate channels. There has been a concern, however, that, during the manufacturing of such devices, ion induced damages to their Si vertical walls may directly affect the device performance<sup>6</sup> since part of such Si vertical walls form the gate channels.

Ion induced damages formed on Si surfaces directly facing ion bombardment during reactive ion etching (RIE) processes were extensively studied for planer MOSFET devices in the past.<sup>7–11</sup> Similarly, during plasma-based gate etching processes of finFETs, energetic ions may hit the vertical walls. However, such ions are highly directional toward the wafer surface, driven by the electric field in the plasma sheath near the material surface. Therefore, incident angles of such ions on Si vertical walls of finFETs are typically grazing, i.e., close to  $90^\circ$  measured from the surface normal. If the vertical wall is tapered, it may be even more subject to such ion bombardment. Damaging effects of energetic ions at a large angle of incidence on the crystalline structure of the surface are often considered to be negligible as it is often assumed that most such ions are reflected by the surface and tend not to be implanted into the material. However, a recent study<sup>6</sup> based on mass-selected ion beam experiments<sup>12</sup> has shown that  $H^+$  ion injection at an incident angle of  $60^\circ$  can

form a deep damage layer near the substrate surface. Although an incident angle of  $60^\circ$  may be still small compared with typical incident angle of grazing ions during gate etching processes of finFET structures, the earlier study suggested a possibility of damage formation by energetic  $H^+$  ions even at grazing incidence. A better understanding of the damage formation mechanisms by light ions such as hydrogen injected into a solid surface with various incident angles would help avoid unexpected damage formation at Si vertical walls during gate etching processes.

Due to the small mass and radius of a hydrogen atom compared with those of a silicon atom, damage formation of Si surfaces by energetic incident  $H^+$  ions<sup>8,9,13</sup> is known to be different from that by heavier incident ions such as  $Ar^+$ . Earlier studies<sup>14–17</sup> on RIE processes by hydrogen containing plasmas recognized Si damage formed by  $H^+$  ion bombardment as a cause of lifetime degradation of metal–oxide–semiconductor capacitors. What has not been discussed so much is a possibility of Si damage formation by energetic ions at oblique angle impact.

In this study, therefore, we attempt to understand the damage formation mechanisms of Si surfaces by ion bombardment at various angles of incidence, using molecular dynamics (MD) simulations. In actual gate etching processes of fin-FET structures, plasmas based on halogen gases such as  $Cl_2$  or HBr are widely used. However, in order to separate the effect of energetic ion impact from chemical effects in a damage formation process in the Si substrate, we use only  $Ar^+$  and  $H^+$  ions in our simulations, assuming that the damage formation mechanism by  $Ar^+$  ions is indicative of that by physical impact of heavy ions (i.e., ions whose masses are comparable with or heavier than that of a Si atom) such as  $Cl^+$  and  $Br^+$ . The goal of this study is, however, to show that energetic impact of relatively large and heavy ions such as  $Ar^+$ ,  $Cl^+$ , and  $Br^+$  on a Si substrate is qualitatively and

<sup>a)</sup>Electronic mail: hamaguch@ppl.eng.osaka-u.ac.jp

significantly different from that by small and light ions such as  $H^+$ . It will be shown in this study that small and light ions such as  $H^+$  can penetrate so much more deeply than larger and heavier ions into a Si substrate and, if their dose is sufficiently high, can cause significant amorphization of Si.

Since a study on injection of simple ions such as  $Ar^+$  or  $H^+$  into Si is so fundamental, it seems widely believed that everything related to the subject, including various data such as sputtering yields, should have been known by now. However, in reality, it is not the case. In the case of the authors, when we examined a possibility of designing a new damage-free processing technology for nanoscale structures of next-generation semiconductor chips, we found it necessary to revisit this problem in order to understand the mechanisms of damage formation in Si by energetic impact of various ions, especially those at large angles of incidence. As we shall discuss later, published literatures on the sputtering yields of Si by energetic  $H^+$  ions are scarce. Even for sputtering yields of Si by energetic  $Ar^+$  ions, there seem very few or possibly no published data of Si sputtering yields by energetic  $Ar^+$  ions as functions of the beam incident angle in a relatively low energy range (e.g., 500 eV or less). Therefore, we believe that our MD simulation results on Si sputtering by  $Ar^+$  and  $H^+$  ion incidence obtained in this study are novel and the first of its kind and help understand the damage formation mechanisms on Si surfaces during RIE processes.

## II. SIMULATION METHODS

In the MD simulation presented in this article, we use Stillinger–Weber type interatomic potential functions,<sup>18–21</sup> similar to those used in earlier simulation studies of Refs. 22 and 23, with newly adjusted parameters. For the sake of simplicity, effects of the electric charges of incident ions are not taken into account in the evaluation of interatomic forces. For example, an energetic incident ion in an actual experiment is treated as a charge-neutral atom with the same kinetic energy in the MD simulation used in this study. This approximation may be justified due to an Auger emission process that neutralizes incident ions immediately before they interact with surface Si atoms.<sup>24,25</sup>

In the simulation, the Si substrate is represented by a rectangular box of crystalline Si with the top surface being Si (100). Its horizontal cross section is a square of  $3.26 \times 3.26$  nm whereas its depth varies depending on the simulation conditions and can be as large as 80 nm. The depth is taken sufficiently large in order to minimize effects of the presence of the artificial bottom surface of the simulation box. To avoid unnecessary downward shift of the substrate during simulation by momentum transfer from energetic ions to the substrate, the bottom layer of the substrate is fixed as an anchor layer. Periodic boundary conditions are imposed in the horizontal directions so that the system would represent an infinitely wide surface layer.

The initial Si substrate is set in thermal equilibrium at a temperature of 300 K. An ion is then injected into the Si substrate surface in the simulation. As in typical classical MD

simulation, trajectories of all atoms are obtained as the simultaneous solutions of Newton's equations of motion for all atoms in the simulation box. The initial horizontal position of each incident ion is determined randomly and its vertical position is set to be 0.5 nm above the substrate surface. After each ion injection, the constant-energy (microcanonical) MD simulation is carried out for 700 fs and then, for the following 300 fs of MD simulation, the system is gradually cooled down to reach its initial temperature of 300 K. A new ion is then injected into this surface and the same simulation procedure is repeated. After sufficiently many repetitions of such an ion injection cycle, the surface roughness reaches its steady state, which would represent the experimentally observable surface roughness under the given ion bombardment conditions.

Under the ion bombardment conditions examined in this study, essential collision dynamics, such as penetration or reflection of the incident ion and dislocation of Si atoms following the ion impact, takes place within the first 700 fs of each simulation cycle. The latter 300 fs cooling simulation<sup>23,26–28</sup> is meant to emulate a natural relaxation process of the surface, which would typically ensue for micro- or milliseconds in reality, before another ion incidence occurs in the same neighboring area (represented by the surface area of the model substrate). Ions used in the simulations are  $H^+$  and  $Ar^+$ , with incident ion energies in the range from 100 to 500 eV and incident ion angles from  $0^\circ$  (normal incidence) to  $80^\circ$ .

In actual gate etching processes by RIE, of course, incident ions typically have a wide energy distribution, depending on the RF bias voltage applied to the electrode that holds the substrate. However, the focus of this study is the damage formation by energetic ion impact, so what matters is whether most energetic ions of our interest in the plasma causes damages on the Si surface or its subsurface bulk region. Therefore, we examine effects of only monoenergetic ion beams on Si surfaces. Furthermore, in actual plasmas, a large number of charge neutral reactive species (i.e., free radicals) can passivate the surface. Although such surface passivation, which typically occurs within the top surface layer of a thickness of 1 nm or so, can significantly affect the sputtering yields, we assume that it hardly affects the orbits of energetic particles that penetrate for tens of nanometers into the Si substrate. Therefore, in the present study, we focus only on beam–surface interactions and defer the surface passivation effects on damage formation to a future study.

## III. SIMULATION RESULTS

Figure 1 shows Si substrate structures obtained from MD simulations after  $Ar^+$  ion injections at incident angles of  $0^\circ$  (normal incidence),  $30^\circ$ ,  $60^\circ$ , and  $80^\circ$ . Here, small spheres represent Si atoms and large spheres represent Ar atoms implanted in the Si substrate. Here, Ar atoms are depicted disproportionately large so that they become more conspicuous. It is seen that there are not many implanted Ar atoms in the cases shown here. The incident  $Ar^+$  ion energy is 500 eV



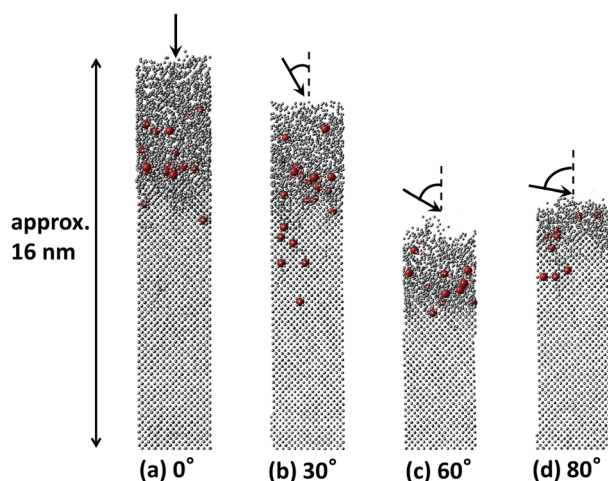


FIG. 1. (Color online) Si substrate structures after 500 eV  $\text{Ar}^+$  ion injections. Small spheres represent Si atoms and large spheres represent Ar atoms implanted in the Si substrate. Here, Ar atoms are depicted disproportionately large so that they become more conspicuous. It is seen that there are not many implanted Ar atoms. The  $\text{Ar}^+$  ion dose is  $7.3 \times 10^{15}/\text{cm}^2$  in each case. The angles of incidence are (a)  $0^\circ$ , i.e., normal incidence, (b)  $30^\circ$ , (c)  $60^\circ$ , and (d)  $80^\circ$ .

and the ion dose was  $7.3 \times 10^{15}/\text{cm}^2$  in each case. The initial top surfaces of all model substrates before ion bombardment were set at the same height and the differences in height in Fig. 1 reflect differences in the etch rate, which depends on the incident angle. It is clearly seen that the etch rate is the largest at  $60^\circ$  among the four cases examined here.

The initial substrate was crystalline Si and it is seen in Fig. 1 the top layer of each model substrate has been damaged (i.e., amorphized) by ion bombardment. The thickness of the amorphized layer clearly depends on the ion incident angle and is the lowest at the largest incident angle.

Suppose that the top substrate surface of Fig. 1 represents a vertical wall of a finFET structure, as schematically depicted in Fig. 2. In a typical gate etching process, most ions accelerated by the sheath voltage travel nearly in

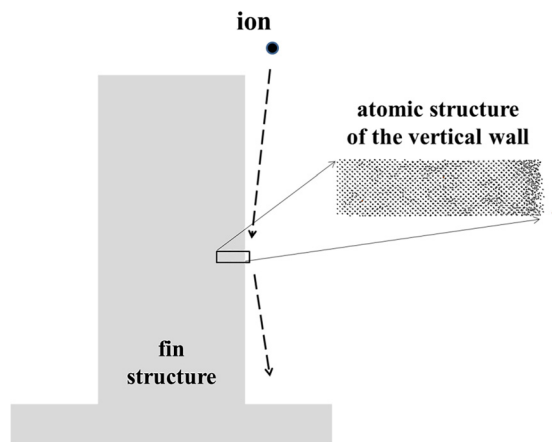


FIG. 2. (Color online) Schematic diagram of a finFET structure, showing the relation of MD simulations in this study with a finFET structure and ions hitting the vertical walls with grazing angles.

parallel to the vertical wall and ions that collide with the surface are most likely to do so at grazing angles. The results of Fig. 1 suggest that damage formed by grazing incidence of  $\text{Ar}^+$  ions (or other ions whose mass is similar to or larger than that of Si, such as  $\text{Cl}^+$  or  $\text{Br}^+$ ) is limited only to a very thin layer at the vertical wall. The observation here obtained from MD simulation is consistent with experimental observation given in Ref. 6, where a transmission electron microscopy image of cross section of a Si sample after 500 eV  $\text{Br}^+$  ion beam bombardment at an oblique angle of incidence ( $60^\circ$ ) exhibits only limited surface layer damage.

Figure 3 shows Si etching yields by  $\text{Ar}^+$  ions of given incident energies as functions of angle of incidence, obtained from MD simulation used for this study. The curves are guides to the eye. Experimentally obtained Si sputtering yields by  $\text{Ar}^+$  ions at normal incidence with various incident energies are summarized in Ref. 29, with which the values at  $0^\circ$  of Fig. 3 are in good agreement. There seem no publicly available experimental data of angle dependent Si sputtering yield by  $\text{Ar}^+$  ions at low incident energy (e.g., 500 eV or lower). Therefore, Fig. 3 presents our best theoretical estimate of Si sputtering yields at oblique angles of incidence.

Figure 4 shows Si substrate structures obtained from MD simulations after  $\text{H}^+$  ion injections at incident angles of  $0^\circ$  (normal incidence),  $30^\circ$ ,  $60^\circ$ , and  $80^\circ$ . Here, gray spheres represent Si atoms and large red spheres represent H atoms. Here, H atoms are depicted disproportionately large so that they become more conspicuous. Note that majority of implanted H atoms are found in a much deeper region, as will be discussed later in this section. The incident  $\text{H}^+$  ion energy was 300 eV, and the ion dose was  $9.4 \times 10^{16}/\text{cm}^2$  in each case. As in Fig. 1, the initial top surfaces of all model substrates before ion bombardment were set at the same height and the differences in height in Fig. 4 reflect differences in the etch rate.

The sputtering yields of Si by  $\text{H}^+$  ion beams are not much known except for the yields at normal incidence experimentally obtained by Roth *et al.*,<sup>30</sup> data of which are also listed in Ref. 29. There seem no publicly available experimental data of angle-dependent Si sputtering yield by  $\text{H}^+$  ions in the energy range of our interest, either. At normal incidence, the experimentally obtained Si sputtering yield by 300 eV  $\text{H}^+$

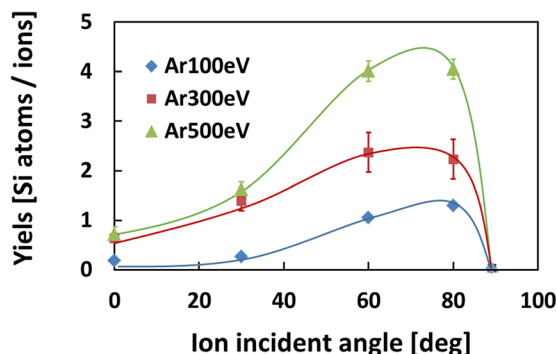


FIG. 3. (Color online) Si etching yields by  $\text{Ar}^+$  ions of given incident energies as functions of angle of incidence, obtained from MD simulations. The curves are guides to the eye.

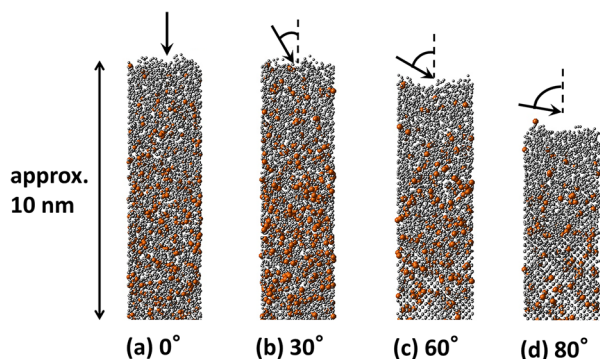


FIG. 4. (Color online) Si substrate structures after 300 eV  $H^+$  ion injections. Small spheres represent Si atoms and large spheres represent H atoms implanted in the Si substrate. Here, H atoms are depicted disproportionately large so that they become more conspicuous. Note that majority of implanted H atoms are found in a much deeper region later. The ion dose is  $9.4 \times 10^{16}/\text{cm}^2$  in each case. The angles of incidence are (a)  $0^\circ$ , i.e., normal incidence, (b)  $30^\circ$ , (c)  $60^\circ$ , and (d)  $80^\circ$ .

ions is approximately  $6 \times 10^{-3}$  whereas the sputtering yield obtained from our MD simulation is about  $10^{-2}$  with a relatively large error bar. Since the sputtering yield is so low under these conditions, accurate evaluation of the sputtering yield (i.e., etch rate) by MD simulation would require spatially larger and temporally longer scale simulation to reduce statistical errors. Therefore, evaluation of Si sputtering yield by  $H^+$  ions by MD simulation is deferred to a future study. However, our preliminary estimates of Si sputtering yields by  $H^+$  ions at normal incidence as well as our evaluation of Si sputtering yields by Ar ions given in Fig. 4 are sufficiently consistent with the corresponding experimental data that are available in literature, which we believe vindicates the reliability of our MD simulation.

It is seen in Fig. 4 that, in the cases of normal and  $30^\circ$  incidence of 300 eV  $H^+$  ions, the damage caused by the ion bombardment is so deep that almost all substrate regions are amorphized. Furthermore, even at  $80^\circ$  incidence, the amorphized Si layer is much deeper than that by (more energetic) 500 eV  $Ar^+$  ion incidence at the same angle of incidence shown in Fig. 1. The simulation results are qualitatively consistent with experimental observations given in Ref. 6, where ion beam experiments have shown that the damaged Si layer thickness due to  $H^+$  ion incidence hardly depends on the angle of incidence.

Figure 5 shows the Si substrate structures after  $H^+$  ion injections at an incident angle of  $80^\circ$  with different ion incident energies, i.e., (a) 500, (b) 300, and (c) 100 eV. The ion dose in each case is the same as that of Fig. 4, i.e.,  $9.4 \times 10^{16}/\text{cm}^2$ . It is seen that more Si atoms are dislocated at higher incident energies.

It should be noted that many incident ions at a large angle of incidence are reflected from the surface. Figure 6 shows the reflection rate of  $H^+$  ions as functions of the incident angle at various incident energies, obtained from MD simulation. A curve shown in Fig. 6 is a guide to the eye. Here, the reflection rate is defined as the ratio of the number of incident  $H^+$  ions that are reflected from the surface to the

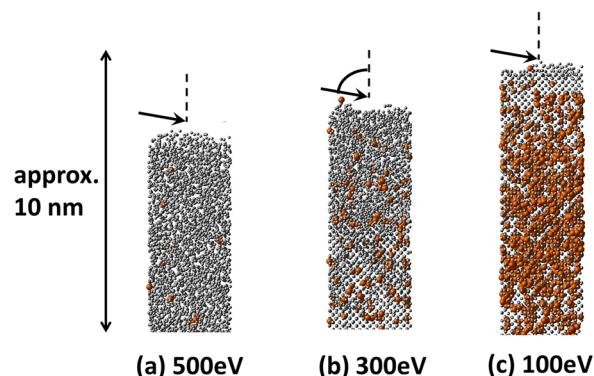


FIG. 5. (Color online) Si substrate structures after  $H^+$  ion injections at an incident angle of  $80^\circ$ . Small spheres represent Si atoms and large spheres represent H atoms implanted in the Si substrate. The ion dose is  $9.4 \times 10^{16}/\text{cm}^2$  in each case. The incident energies are (a) 500 eV, (b) 300 eV, and (c) 100 eV.

total number of incident  $H^+$  ions. It is seen that the reflection rate hardly depends on the incident energy among the cases examined here. At a large incident angle, only a small fraction of incident ions enter the substrate, which explains lower densities of dislocated Si atoms at larger incident angles in Fig. 4. In Fig. 4, it is seen that the amorphized layer observed at  $80^\circ$  is shallower than those at smaller incident angles. However, this does not mean that crystalline Si below the amorphized layer is completely intact. Unlike  $Ar^+$  ions, some incident  $H^+$  ions can penetrate deeply into the substrate even at a large angle of incidence and can dislocate Si atoms at large depths.

Figure 7 shows density profiles of H atoms implanted in Si substrates after the substrates are subject to 500 eV  $H^+$  ion incidence at incident angles of  $0^\circ$  (normal incidence),  $30^\circ$ ,  $60^\circ$ , and  $80^\circ$ . The dose is  $2.8 \times 10^{16}/\text{cm}^2$  in each case. The simulations were performed with sufficiently deep model substrates and the H density plotted in Fig. 7 is the average over a layer of 2 nm at each depth. It should be noted that the depth profiles were plotted over a much larger depth in Fig. 7 than those shown in Figs. 1, 4, and 5. (However, the ion dose in Fig. 7 is about three times smaller than those of

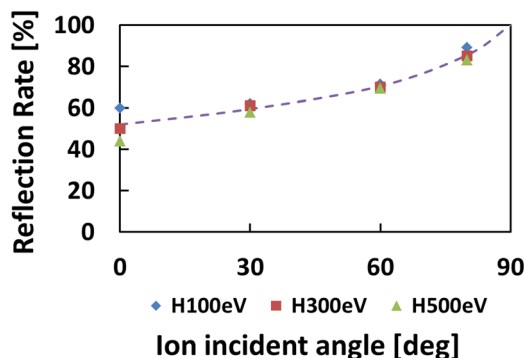


FIG. 6. (Color online) Reflection rates of  $H^+$  ions incident on Si substrates as functions of the incident angle at three different incident energies: 100, 300, and 500 eV, obtained from MD simulation. The curves are guides to the eye.

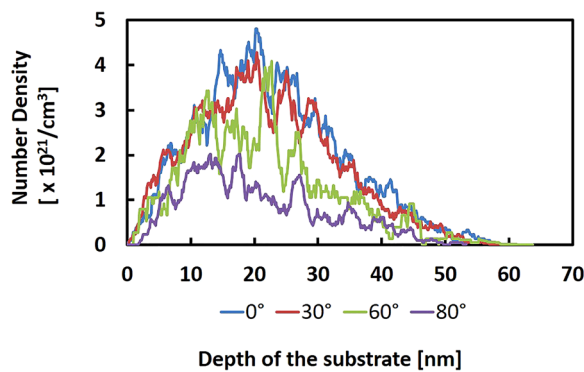


Fig. 7. (Color online) Density profiles of H atoms implanted in Si substrates after the substrates are subject to 500 eV  $H^+$  ion incidence at incident angles of  $0^\circ$  (normal incidence),  $30^\circ$ ,  $60^\circ$ , and  $80^\circ$ . The ion dose is  $2.8 \times 10^{16}/\text{cm}^2$  in each case. The density is the average over a layer of 2 nm at each depth.

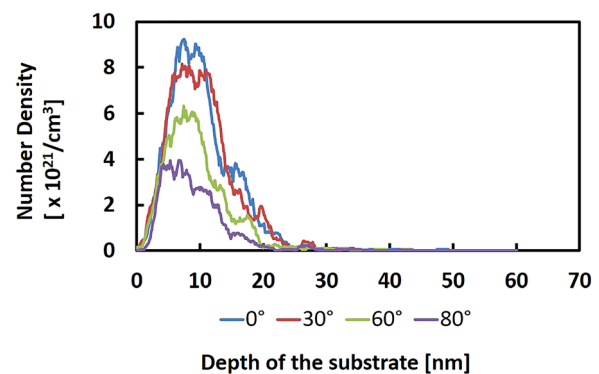


Fig. 8. (Color online) Density profiles of H atoms implanted in Si substrates after the substrates are subject to 100 eV  $H^+$  ion incidence at incident angles of  $0^\circ$  (normal incidence),  $30^\circ$ ,  $60^\circ$ , and  $80^\circ$ . The ion dose is  $2.8 \times 10^{16}/\text{cm}^2$  in each case. The density is the average over a layer of 2 nm at each depth.

Figs. 1, 4, and 5. Simulations to obtain profiles such as those in Fig. 7 with deeper model substrates take significantly longer computational time than those to obtain Figs. 1, 4, and 5, which were obtained with much shallower model substrates.) Since the MD simulation used in this study does not simulate long-time diffusion processes of H atoms in Si, Fig. 7 presents the hydrogen density profiles “as implanted.” In reality, significant hydrogen diffusion in Si can take place with such large density gradients and the stable density profiles of implanted H in Si may have lower peak densities and broader depth profiles.

Oehrlein and Lee<sup>8</sup> examined deuterium (rather than hydrogen, for the sake of measurement) profiles in Si using secondary ion mass spectroscopy after the Si substrates were etched in RIE processes with  $\text{CF}_4$  and  $\text{D}_2$  gases. Their measurements showed that the implanted deuterium concentration can reach  $10^{21} \text{ cm}^{-3}$  and the profile of significantly high deuterium concentrations ( $10^{19} \text{ cm}^{-3}$  or higher) can extend to 50–100 nm in depth under typical RIE process conditions. Although the experimental conditions of Ref. 8 are very different from the ion beam conditions we used in this MD simulation study and significant diffusion of deuterium was also suggested to account for the experimental observations, the experimentally obtained deuterium profiles given in Ref. 8 suggest that the as-implanted hydrogen concentration profiles with tens of nanometers shown in Fig. 7 are not implausible under typical processing conditions.

It is clearly seen in Fig. 7 that the maximum depth reachable by incident H atoms hardly depends on the angle of incidence for the given incident energy. It is also seen that the implanted H atomic density in the Si substrate is lower at a higher angle of incident. This is because, as seen in Fig. 6, for a given incident ion dose ( $2.8 \times 10^{16}/\text{cm}^2$  in each case of Fig. 7), more incident ions are reflected and do not enter the Si substrate at larger incident angles.

Similarly Fig. 8 shows the density profiles of H atoms implanted in Si substrates after the substrates are subject to 100 eV  $H^+$  ion incidence at incident angles of  $0^\circ$  (normal incidence),  $30^\circ$ ,  $60^\circ$ , and  $80^\circ$ . The dose is  $2.8 \times 10^{16}/\text{cm}^2$  in

each case. The H density plotted in Fig. 8 is the average over a layer of 2 nm at each depth.

The results of both Figs. 7 and 8 indicate that, even at large angles of incidence, incident H atoms can penetrate as deeply as incident H atoms at normal incidence and therefore the maximum depth of damaged (i.e., dislocated) Si by H ion injection may hardly depend on the angle of incidence if the ion dose is sufficiently large.

#### IV. CONCLUSIONS AND SUMMARY

Damage of a crystalline Si substrate, i.e., dislocation of Si atoms from their original crystalline positions, caused by ion bombardment at various incident angles has been examined with the use of MD simulations. The goal of this study is to assess possible damage formation on vertical wall surfaces of finFET structures during gate etching processes, where the Si vertical walls may be subject to grazing incidence of energetic ions. Since part of the Si vertical walls of a finFET can form a conductive channel of the device, damage to the vertical walls may adversely affect the device performance. In typical gate etching processes, plasmas based on HBr are widely used, where  $H^+$  and  $\text{Br}^+$  ions are likely to be some of the major incident ionic species. In this study, we examined damage formation on a crystalline Si surface by  $H^+$  and  $\text{Ar}^+$  ions, assuming that the damage formation mechanism by  $\text{Ar}^+$  ions is indicative of that by physical impact of heavy ions (i.e., ions whose masses are comparable with or heavier than that of a Si atom) such as  $\text{Cl}^+$  and  $\text{Br}^+$ .

It has been found from our MD simulation that the thickness of a Si damaged layer caused by energetic  $\text{Ar}^+$  ion incidence decreases with the angle of incidence, indicating that damage formation on Si vertical walls by grazing incidence of heavy ions such as  $\text{Ar}^+$ ,  $\text{Cl}^+$ , or  $\text{Br}^+$ , is likely to be negligible during gate etching processes of finFET structures. This is because most ions of grazing incidence are reflected from the surface and, if some ions enter the substrate, they leave damage only in a very thin layer at the surface.

However, it has been also found that the thickness of a Si damaged layer caused by energetic  $H^+$  ion incidence hardly



depends on the angle of incidence, indicating that grazing incidence of  $H^+$  ions may cause some damage to the Si vertical walls during gate etching processes of finFETs. This is because  $H^+$  ions can scatter in a wide range of directions once they enter the substrate and travel deeply into the substrate due to their small mass and atomic radius.

The simulation results are consistent with earlier observations of damage formation on Si surfaces performed in ion beam experiments of Ref. 6, which shows that the depths of amorphized layers of Si substrates formed by 500 eV  $H^+$  ions with a dose of  $1.0 \times 10^{17} \text{ cm}^{-2}$  at normal and  $60^\circ$  angle of incidence are essentially the same. Accurate measurements of surface properties, such as sputtering yields or damage formation, for a surface subject to ion bombardment of grazing incidence are in general difficult to perform since it requires highly accurate beam positioning and high beam stability. Our study based on MD simulation has not only confirmed the consistency of simulation results with earlier experimental observations for damage formation up to  $60^\circ$  angle of incidence but also indicated that energetic impact of  $H^+$  ions on Si surface can damage the surface up to a similar depth even when the angle of incidence is as large as  $80^\circ$ .

In summary, the damage formation mechanism by incidence of  $H^+$  ions on a Si surface is different from that by incidence of  $Ar^+$  ions due to their smaller mass and atomic radius. Energetic H atoms do not lose much kinetic energy when they collide with Si atoms of the substrate due to the large difference in mass between Si and H. Also, energetic H atoms can travel deeply into the Si substrate due to their relatively small atomic radius compared with the size of interstitial space of Si. Furthermore traveling H atoms in a Si solid may scatter with large angles at collisions with Si atoms, which results in a wide range of directions in which incident H atoms travel after they enter the Si substrate regardless of their angles of incidence. This contrasts starkly with the case of heavier atoms, such as Ar, Cl, or Br, whose atomic radii are comparable with that of Si. Such ions cannot penetrate deeply into the Si substrate especially when they hit the substrate surface at large angles of incidence and therefore tend to form a relatively shallow layer of dislocated Si by ion impact.

The results obtained in this study suggest that, in gate etching processes with HBr plasmas or other plasmas that contain hydrogen, control of energetic hydrogen ion bombardment is critical in minimizing possible surface damage at Si vertical walls.

## ACKNOWLEDGMENT

The work was partially supported by Grants-in-Aid for Scientific Research from Ministry of Education, Culture, Sports, Science and Technology (MEXT), Japan.

- <sup>1</sup>Y.-K. Choi, N. Lindert, P. Xuan, S. Tang, D.-W. Ha, E. Anderson, T.-J. King, J. Bokor, and C. M. Hu, *IEEE Int. Electron Devices Meet., Tech. Dig.* **2001**, 421.
- <sup>2</sup>J. Kedzierski, M. Jeong, E. Nowak, T. S. Kanarsky, Y. Zhang, R. Roy, D. Boyd, D. Fried, and H.-S. P. Wong, *IEEE Trans. Electron Devices* **50**, 952 (2003).
- <sup>3</sup>T. Skotnicki, J. A. Hutchby, T.-J. King, H.-S. P. Wong, and F. Boeuf, *IEEE Circuits Devices Mag.* **21**, 16 (2005).
- <sup>4</sup>J.-P. Colinge, *FinFETs and Other Multi-Gate Transistors* (Springer, New York, 2007).
- <sup>5</sup>I. Ferain, C. A. Colinge, and J.-P. Colinge, *Nature* **479**, 310 (2011).
- <sup>6</sup>T. Ito, K. Karahashi, K. Mizotani, M. Isobe, S.-Y. Kang, M. Honda, and S. Hamaguchi, *Jpn. J. Appl. Phys., Part 1* **51**, 08HB01 (2012).
- <sup>7</sup>S. W. Pang, D. D. Rathman, D. J. Silversmith, R. W. Mountain, and P. D. DeGraff, *J. Appl. Phys.* **54**, 3272 (1983).
- <sup>8</sup>G. S. Oehrlein and Y. H. Lee, *J. Vac. Sci. Technol., A* **5**, 1585 (1987).
- <sup>9</sup>S. J. Jeng, G. S. Oehrlein, and G. J. Scilla, *Appl. Phys. Lett.* **53**, 1735 (1988).
- <sup>10</sup>M. Tuda, K. Shintani, and J. Tanimura, *Appl. Phys. Lett.* **79**, 2535 (2001).
- <sup>11</sup>T. Ohichi, S. Kobayashi, M. Fukasawa, K. Kugimiya, T. Kinoshita, T. Takizawa, S. Hamaguchi, Y. Kamide, and T. Tatsumi, *Jpn. J. Appl. Phys., Part 1* **47**, 5324 (2008).
- <sup>12</sup>K. Karahashi and S. Hamaguchi, *J. Phys. D: Appl. Phys.* **47**, 224008 (2014).
- <sup>13</sup>W. K. Chu, R. H. Kastl, R. F. Lever, S. Mader, and B. J. Masters, *Phys. Rev. B* **16**, 3851 (1977).
- <sup>14</sup>R. G. Frieser, F. J. Montillo, N. B. Zingerman, W. K. Chu, and S. R. Mader, *J. Electrochem. Soc.* **130**, 2237 (1983).
- <sup>15</sup>X. C. Mu, S. J. Fonash, A. Rohatgi, and J. Rieger, *Appl. Phys. Lett.* **48**, 1147 (1986).
- <sup>16</sup>R. W. Collins, B. G. Yacobi, K. M. Jones, and Y. S. Tsuo, *J. Vac. Sci. Technol., A* **4**, 153 (1986).
- <sup>17</sup>T. Ito, K. Karahashi, M. Fukasawa, T. Tatsumi, and S. Hamaguchi, *Jpn. J. Appl. Phys., Part 1* **50**, 08KD02 (2011).
- <sup>18</sup>F. H. Stillinger and T. A. Weber, *Phys. Rev. B* **31**, 5262 (1985).
- <sup>19</sup>F. H. Stillinger and T. A. Weber, *J. Chem. Phys.* **88**, 5123 (1988).
- <sup>20</sup>F. H. Stillinger and T. A. Weber, *Phys. Rev. Lett.* **62**, 2144 (1989).
- <sup>21</sup>T. A. Weber and F. H. Stillinger, *J. Chem. Phys.* **92**, 6239 (1990).
- <sup>22</sup>H. Ohta and S. Hamaguchi, *J. Chem. Phys.* **115**, 6679 (2001).
- <sup>23</sup>H. Ohta and S. Hamaguchi, *J. Vac. Sci. Technol., A* **19**, 2373 (2001).
- <sup>24</sup>D. W. Hess, *J. Vac. Sci. Technol., A* **8**, 1677 (1990).
- <sup>25</sup>H. D. Hagstrum, *Phys. Rev.* **96**, 336 (1954).
- <sup>26</sup>H. J. C. Berendsen, J. P. M. Postma, W. F. van Gunsteren, A. DiNola, and J. R. Haak, *J. Chem. Phys.* **81**, 3684 (1984).
- <sup>27</sup>P. H. Hünenberger, *Adv. Polym. Sci.* **173**, 105 (2005).
- <sup>28</sup>K. Miyake, T. Ito, M. Isobe, K. Karahashi, M. Fukasawa, K. Nagahata, T. Tatsumi, and S. Hamaguchi, *Jpn. J. Appl. Phys., Part 1* **53**, 03DD02 (2014).
- <sup>29</sup>Y. Yamamura and H. Tawara, *At. Data Nucl. Data Tables* **62**, 149 (1996).
- <sup>30</sup>J. Roth, J. Bohdansky, and W. Ottenberger, Report IPP9/26, Institute of Plasma Physics, Garching, Germany (1979).